A. Chub, O. Korkh, R. Kosenko and D. Vinnikov,

" Novel Approach Immune to Partial Shading for Photovoltaic Energy Harvesting from Building Integrated PV (BIPV) Solar Roofs "

20th European Conference on Power Electronics and Applications
EPE'18 ECCE Europe. Riga 17th-21st September 2018.

Novel Approach Immune to Partial Shading for Photovoltaic Energy Harvesting from Building Integrated PV (BIPV) Solar Roofs

Andrii Chub[1], Oleksandr Korkh[1], Roman Kosenko[2], Dmitri Vinnikov[1,2]

[1]TALLINN UNIVERSITY OF TECHNOLOGY
Ehitajate tee 5
Tallinn, Estonia
Tel.: +372 620 3702
E-Mail: {andrii.chub, oleksandr.korkh}@ttu.ee
URL: http://www.ttu.ee/en

[2]UBIK SOLUTIONS OÜ
Regati Pst. 1
Tallinn, Estonia
Tel.: +372 639 5500
E-M ail: {roman, dmitri}@ubiksolutions.eu
URL: http://www.ubiksolutions.eu

Acknowledgments

This research was supported by the Estonian Centre of Excellence in Zero Energy and Resource Efficient Smart Buildings and Districts, ZEBE, grant 2014-2020.4.01.15-0016 funded by the European Regional Development Fund and by the Estonian Research Council (project PUT1443).

Keywords

Renewable energy systems, photovoltaic, single-phase system, Z-source converter, generation of electric energy.

Abstract

The rapid development of solar photovoltaic (PV) technology facilitates implementation of building integrated PV (BIPV) as a key technology for energy efficient buildings. This study addresses parallel grid integration of microstrings composed of BIPV modules. Existing BIPV products are reviewed. A low number of PV cells per module suggests their series connection to be compatible with microinverters. A concept of a shade tolerant microinverter called Optiverter was applied to BIPV microstrings and compared experimentally to a high-end and a low-end commercial microinverters. Several shading scenarios for three BIPV element types were considered. The Optiverter was compared to several commercial microinverters in terms of maximum power point tracking under unshaded and shaded conditions, power conversion efficiency, maximum power point tracking efficiency, and overall efficiency combining these two parameters.

Introduction

In the last decades, numerous challenges of sustainable and efficient energy generation, transportation, consumption and storage were resolved by researchers and developers, which involve the high impact of power electronics technologies [1]-[3]. One of the main bottlenecks that limits the sustainable development of the society is energy efficiency of the buildings [4], [5] since they constitute more than 40% of the electricity consumption in the EU and USA [6], [7]. Therefore, European Commission released Energy Performance of Buildings Directive that requires all new buildings commissioned after the year 2020 to comply with national requirements for nearly zero energy buildings (NZEBs) [7], [8]. The directive imposes strict limitations that complicate the construction of the residential and small commercial buildings. It was modified in April 2018 to include the requirement of on-site infrastructure for charging of electric vehicles. Moreover, California Energy Commission introduced rooftop solar mandate in May 2018, which requires all new residential buildings to include rooftop PV installations. It is expected to drive local PV market in the following decade.

On-site energy generation can reduce the energy consumption footprint of a building down to the level acceptable for the NZEBs [8]. However, energy production facilities for the buildings are limited, and residential power system design could utilize PV generation, fuel cell electricity back-up or combined

heat and power (CHP) systems, energy storage, micro wind turbines, vehicle-to-grid interface converters, etc. [9], [10]. Rooftop PV installations are a typical application of the renewable energy in the residential systems due to ample solar irradiance [11]. Conventional string inverters handling PV modules connected in series or multilevel converters could be used for BIPV grid integration despite their low performance at partial shading of PV modules, limited scalability and reliability [12], [13]. Hence, the parallel grid integration of PV modules by means of the microinverters was introduced [14]-[16]. They feature high installation flexibility and scalability as well as improve the overall system redundancy, tolerance to shading conditions and failure of individual modules. The novel class of shade tolerant microinverters called the Optiverter introduced recently [17] possesses an ultra-wide input voltage regulation range and, by this means, enables energy harvesting from a PV module under heavily shaded conditions.

The modern residential PV systems are advancing towards building-integrated PV (BIPV) approach when a small PV module is an integral part of a roof, facade or even window and, in this way, replacing conventional construction elements. For BIPV solar roofs, a PV module is produced mechanically and aesthetically compatible with a certain typical roof tile, slate or shingle. As a result, there are plenty of different BIPV roofing systems available with the number of PV cells per construction element between one and twenty four. However, today reports on the technology of their grid integration are virtually unavailable. Application of a string inverter in solar roofs is a possible solution that has limited overall reliability and PV roof design flexibility. Moreover, residential PV applications could face a variety of shading scenarios, like shade from trees or chimney, opaque shading from fallen leaves or snow, bird droppings, unfavorable roof orientations, etc.

This study proposes the parallel integration of microstrings composed of several BIPV modules connected in series, resulting in the open circuit voltage compatible with the microinverters. Here, a shade tolerant microinverter (STMI) can provide a substantial increase in energy production under shaded conditions and can adopt wider selection of configurations, i.e., different number of PV modules connected in series within a microstring is feasible, which distinguishes the STMI from the mass-produced counterparts with a limited range of maximum power point tracking (MPPT). The microinverter with an input voltage range of 8 V to 60 V is used and compared to a low-end microinverter (LoMI) and a high-end microinverter (HiMI) available off-the-shelf and targeting typical 60- and 72-cell Si PV modules. Several shading scenarios for three basic types of the BIPV modules were studied to show the fundamental difference between the microinverters under study by means of the PV energy conversion efficiency that is a product of the power part efficiency and the MPPT efficiency.

Solar PV microinverter and Optiverter technologies

This study compares the performance of three microinverters when operating with a PV microstring composed of several BIPV roofing elements: shade-tolerant microinverter (STMI) called Optiverter [17], low-end microinverter (LoMI) and a high-end microinverter (HiMI) available off-the-shelf. Their parameters are compared in Table I. It is worth mentioning that the LoMI and the HiMI use the same topology containing two interleaved flyback converter feeding a grid-side unfolder stage, as shown in Fig. 1. This topology can perform MPPT only in a narrow voltage range to avoid efficiency penalties. However, the HiMI features higher efficiency resulting from advanced materials and improved overall design, as well as the enhanced maximum power point tracking (MPPT) algorithm with a variable step.

A generalized power circuit block diagram of the PV Optiverter is presented in Fig. 2. The front-end quasi-Z-source series resonant DC-DC converter performs maximum power point tracking (MPPT) and voltage matching between the PV module and the high-voltage DC-link of 400 V. To achieve a wide input voltage regulation range, the front-end converter utilizes the multi-mode control principle [17]. The front-end converter topology harnesses quasi-Z-source network along with the series resonant tank, which allows realization of the buck-boost functionality in a single switching stage.

The distinguishing feature of the STMI is the capability to track global maximum power point (MPP) under any shading conditions by means of scanning of the P-V curve of a PV module or microstring. The STMI control system performs shade-tolerant MPPT (STMPPT) by PV curve sweep shown in Fig. 3. The routine of the STMPPT comprises the global MPPT (GMPPT) and the local MPPT (LMPPT). The former is essentially P-V curve scanning, enabled by the wide input voltage range of the front-end DC-DC converter. During the GMPPT scanning, a number of MPPs are identified. Out of them, only one is the global MPP (GMPP), and all the others are local MPPs (LMPPs). The GMPP data are used to preset the LMPPT routine when the converter moves the operating point near the GMPP. The LMPPT could utilize any conventional or advanced algorithm for performing perturbation near the GMPP. There are two criteria resulting in GMPPT relaunch: the last GMPPT scanning was performed for 30 min before or the power tracked by the LMPPT changes by more than 20%. By these means, the STMI adapts to changes of the shading conditions or the weather. Before the GMPPT rescanning, the STMI is gradually preset to the operating point near the open circuit voltage.

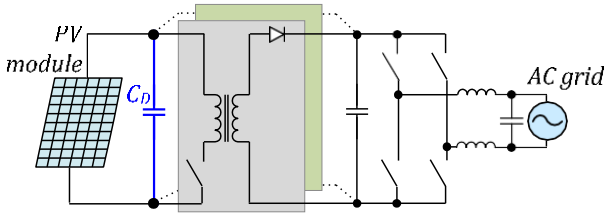

Fig. 1: Typical microinverter topology containing interleaved flyback stage and unfolding inverter.

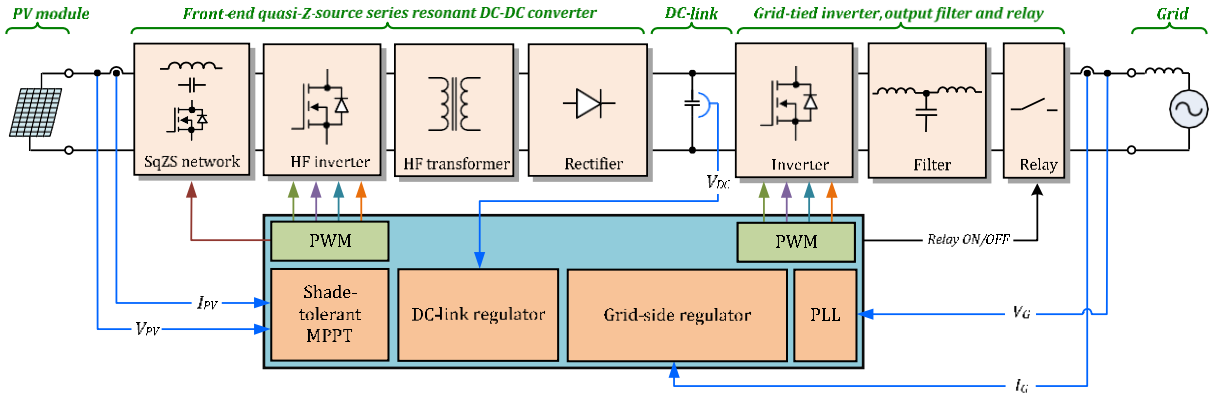

Fig. 2: Generalized power circuit block diagram of the STMI (PV Optiverter).

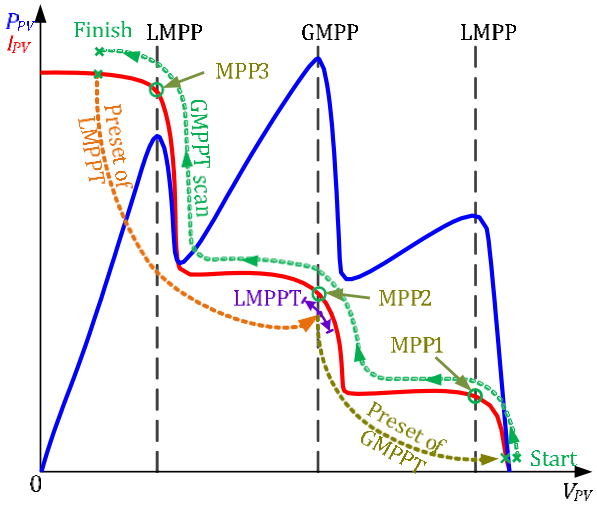

Fig. 3: Idealized sketches of shade-tolerant MPPT implemented in STMI.

The hardware implementation of the STMI is shown in Fig. 4*a*. It features unification of magnetic cores (RM14 are used), integrated control and WiFi communication. The efficiency of the microinverters presented in Table I was measured experimentally by means of Yokogawa WT1800 and a solar array simulator (SAS) Agilent E4360A. The latter was used to emulate PV module with MPP voltage of 33 V. The obtained results in Fig. 4*b* show that STMI is comparable in performance to the counterparts since the commercial HiMI and LoMI feature efficiency in closed loop operation lower than that indicated in their datasheets.

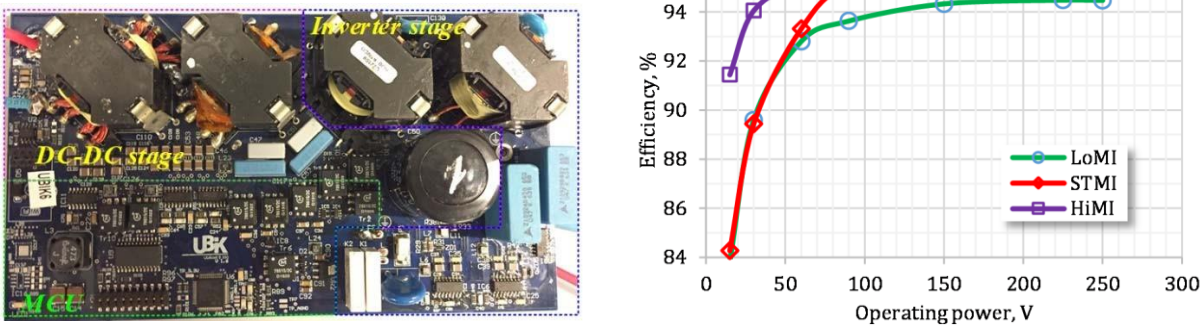

(a) *(b)*

Fig. 4: Hardware implementation of the STMI (a) and efficiency of the microinverters under study (b).

Table I: Parameters of the microinverters under study

Parameter	**Microinverter**		
	LoMI	HiMI	STMI
Maximum DC power, [W]	250	250	350
Absolute input voltage range, [V]	18…54	16…60	6…60
Min/Max starting voltage, [V]	22/-	22/48	6/60
Peak power tracking range, [V]	28…42	27…48	8…48
Measured CEC weighted efficiency @ 33 V, [%]	94.1	95.1	94.8
Measured European weighted efficiency @ 33 V, [%]	93.5	95.2	94.3
Enclosure environmental rating	IP65	IP67	
Communication	PowerLine		WiFi

Technology of BIPV solar roofs

The BIPV solar roof modules are usually built to be compatible with a certain typical roofing technology, like tiles, shingles, or slates. However, most of them use just several types of solar cells encapsulated in a mechanically appropriate frame. A short overview of commercial BIPV roofing products is given in Table II. It compares 13 different BIPV modules in terms of MPP current (I_{MP}), short-circuits current (I_{SC}), MPP voltage (V_{MP}), open circuit voltage (V_{OC}), and power (P) in standard test conditions (STC) with solar radiation of 1000 W/m^2 and cell temperature of 25 °C. Evidently, a BIPV roofing element can contain from 2 to 24 PV cells. Moreover, these elements could be connected in series to create a BIPV rooftop microstring that matches input voltage requirements of a

microinverter. Fig. 5 shows a possible configuration of the PV microstring considering BIPV roofing module types from Table II. Moreover, it shows operation range limits of the microinverters taken into consideration in this study. The STMI can adapt a much wider selection of possible PV microstring configurations owing to its wide input voltage range. This results in design flexibility of BIPV solar roofs, especially if the roof structure is complicated. However, this technology is not limited to the BIPV solar roofs and could be reutilized in the emerging field of BIPV solar facades.

Figure 5 was derived through linear scaling of the data from Table II to show how parameters of a microstring change with a number of BIPV modules connected in series. The tabulated lines tend to follow two major trends in efficiency. Even though it is not clearly stated in datasheets, it is worthwhile assuming that higher efficiency is achieved with monocrystalline silicon (Si) technology, while the polycrystalline Si cells with lower efficiency define the other efficiency trend. Also, Si-based technology was assumed in all the products in Table II since open circuit voltage is in the range between 0.6 V and 0.7 V per cell for all of them. Utilization of Si-based technology is logical, considering its maturity, long-term reliability, and high availability on the market. Usually, Si-based PV cells are produced in the typical size of 156 × 156 mm^2. Use of the typical cell size could be deduced from datasheets of BIPV modules when it is not limited by size constraints dictated by a roofing technology. However, this limitation could be relieved by utilization of an emerging technology of half-cut cells.

Table II: Commercial BIPV modules

Model/Producer	Type	Cells	STC parameters					Exposed area [mm × mm]
			I_{MP} [A]	V_{MP} [V]	I_{SC} [A]	V_{OC} [V]	P [W]	
ZEP B.V. Solar	Tile	2	9	1	9.4	1.2	9	172 × 340
Atlantis Sunslates5	Slate	6	5.08	2.95	5.48	3.78	15	400 × 305
IST SunTegra Tile	Tile	16	8.11	8.26	8.77	10.27	67	355 × 1321
Gaia GS Integra Line SP 595	Shingle	9	8.35	4.8	8.89	6.21	40	595 × 595
CertainTeed Solar Apollo II Tile	Tile	14	8.67	7.27	9.25	9.28	63	438 × 1168
Heda Solar	Tile	2	7.78	1.04	8.31	1.23	8	375 × 285
United Solar	Shingle	18	1.9	9	2.4	13	17	305 × 2195
Sunpower Suntile	Tile	22	5.25	12	5.65	14.6	63	432 × 1500
IST SunTegra Shingle	Shingle	24	8.3	12.65	9.06	15.39	105	500 × 1321
SHARP	Tile	18	7	8.5	7.8	10.65	60	396 × 1499
CertainTeed Solar Apollo II	Shingle	14	8.67	7.27	9.25	9.28	63	448 × 1168
Solarcentury C21e	Slate	18	5.23	9	5.52	11.2	47	318 × 1174
GB-Sol	Slate	12	5.46	6.2	5.77	7.76	35	980 × 410

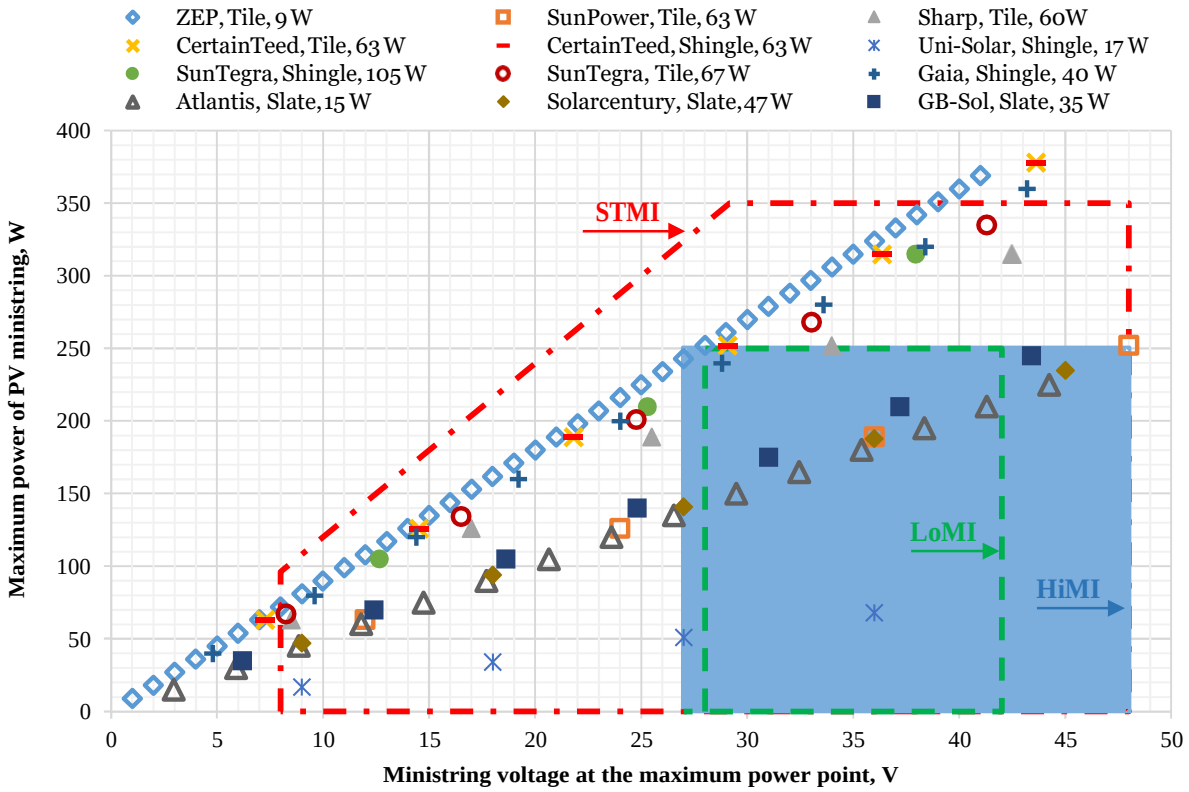

Fig. 5: Possible configuration of the BIPV solar roof microstring based on different BIPV roofing elements, with allowed operating range of the three microinverters considered.

Case study P-V profiles

Three types of BIPV roofing elements (modules) were taken for the further experimental study:

1. Microstring of 8 × Gaia GS Integra Line SP 595 (each module contains 9 typical 156×156 mm^2 PV cells).
2. Microstring of 3 × SunTegra® Shingle (each module contains 24 typical 156×156 mm^2 PV cells).
3. Microstring of 6 × GB-Sol PV Slate (probably contains 12 PV cells - cell size or number is not specified in the datasheet).

To investigate performance under shading conditions, several P-V profiles shown in Figs. 6-8 were synthesized and tabulated for further configuration of SAS Agilent E4360A used in this study. Among these profiles, the profile ST-1 was constructed to show a situation when the highest power is achieved at the lowest voltage (MPP3), while the second local MPP features slightly lower power but twice higher voltage (MPP2) that will result in considerably higher efficiency. The developed STMI (PV Optiverter) handles this situation owing to postprocessing of data acquired during the GMPPT scanning by means of application of the efficiency look-up table. As a result, STMI will prefer operation in the second maximum (MPP2) where it can inject higher power into the grid.

Experimental results

Two operating profiles that correspond to different shading scenarios were simulated for each of the BIPV element type listed above by the solar array simulator Agilent E4360A. The test power profiles are presented in Figs. 6-8. This study considers the overall efficiency of the PV microstring energy conversion η_{PV} as a product of the MPPT efficiency η_{MPPT} and the microinverter efficiency η_{MI}, where $\eta_{PV} = \eta_{MPPT} \times \eta_{MI}$. Definitions of these efficiency values yield from the recommendations of the standard EN 50530:2010 "Overall efficiency of photovoltaic inverters":

$$5_{MPPT} = \frac{P_{DC}}{P_{MPP}} \quad (1)$$

$$5_{MPPT} = \frac{P_{AC}}{P_{DC}} \quad (2)$$

where P_{MPP} is the maximum PV power available from the simulator (corresponds to the global MPP in the given case), P_{DC} is the average input DC power, and P_{AC} is the average output AC power. The DC and AC average powers were measured by the precision power analyzer Yokogawa WT1800. The MPPT efficiency that is the ratio between the PV power captured by a microinverter to the maximum PV power available was verified using internal measurements of the SAS E4360A. In all tests, the microinverters under study were injecting power into the distribution grid with nominal voltage of 230 V and nominal frequency of 50 Hz.

The experimental measurements for the given six PV power profiles are presented in Table III. The STMI features the best performance regarding the PV energy conversion efficiency under partial shading conditions in a BIPV microstring. However, the HiMI can catch the global MPP sometimes owing to the utilization of the variable step MPPT, like in the case of power profiles G-1 and GBS-2, which is infeasible with the LoMI that features a simpler control system. The control system performs overall efficiency optimization using a look-up table of the STMI efficiency. As a result, the STMI operates at MPP2 instead of MPP3 in the case of ST-1 P-V profile since the former features twice higher voltage and power that is less than 2%, lower than that in MPP3. Hence, MPP2 was selected by the

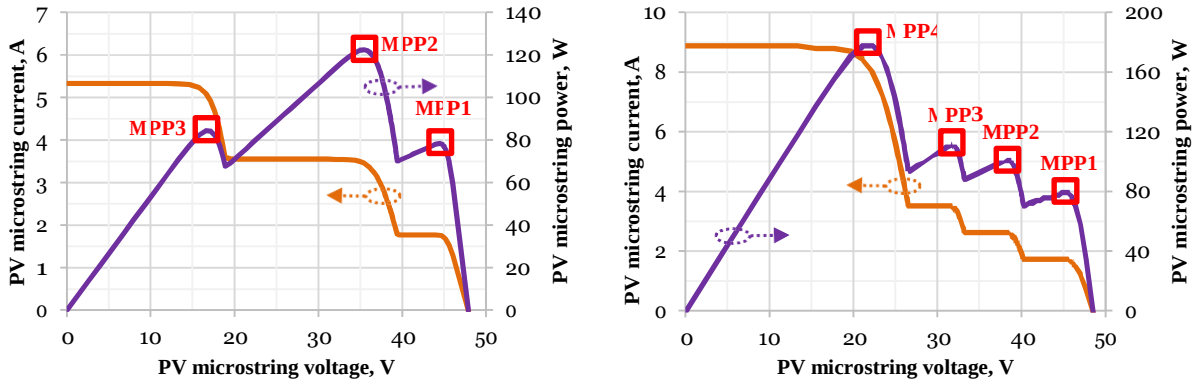

(a) *(b)*

Fig. 6: Power profiles of a shaded microstring composed of 8 × Gaia GS Integra Line SP 595 BIPV modules: (a) G-1: 1 module at 800 W/m^2, 3 modules at 600 W/m^2, 3 modules at 600 W/m^2, 1 module at 200 W/m^2; (b) G-2: 5 modules at 1000 W/m^2, 1 module at 400 W/m^2, 1 module at 300 W/m^2, 1 module at 200 W/m^2.

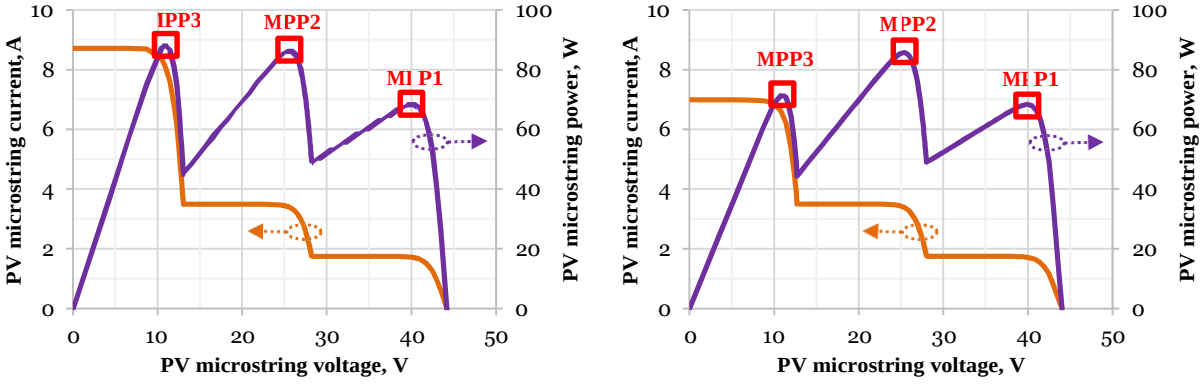

(a) *(b)*

Fig. 7: Power profiles of a shaded microstring composed of 3 × SunTegra® Shingle BIPV modules: (a) ST-1: 1 module at 1000 W/m^2, 1 module at 400 W/m^2, 1 module at 200 W/m^2; (b) ST-2: 1 module at 800 W/m^2, 1 module at 400 W/m^2, 1 module at 200 W/m^2.

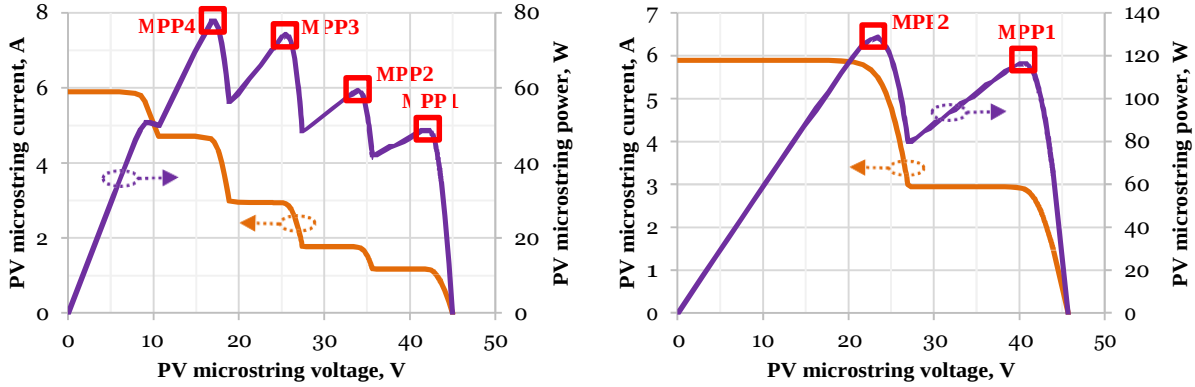

Fig. 8: Power profiles of a shaded microstring composed of 6 × GB-Sol PV Slate BIPV modules: (a) GBS-1: 2 modules at 1000 W/m^2, 1 module at 800 W/m^2, 1 module at 500 W/m^2, 1 module at 300 W/m^2, 1 module at 200 W/m^2; (b) GBS-2: 4 modules at 1000 W/m^2, 2 modules at 500 W/m^2.

control system as more advantageous in terms of AC power injected into the grid. This intelligent control results in an optimal energy yield and lower thermal cycling of the STMI, which should improve the long-term reliability.

Also, additional measurements of the STMI efficiency were performed under different configurations of the BIPV microstring for the three types of the BIPV modules selected. The results shown in Table IV prove the high scalability of the STMI (PV Optiverter) that is capable of delivering PV power to the distribution grid with the efficiency above 80% even at the BIPV microstring voltage level that is three times lower than the minimum MPPT voltage of the commercially available microinverters.

To show the main difference between the MPPT methods used in the microinverters under study, start-up and subsequent MPPT processes were captured (Fig. 9). It is evident that the STMI performs scanning for the global MPP and then goes to the point identified. The STMI is gradually decreasing the operating voltage till it achieves the minimum value of 8 V, defined as the lower limit of the MPPT range. Then, the front-end converter is being preset to the operating point near the global maximum power point. Finally, the LMPPT is activated to track the GMPP. However, scanning time is longer due to the necessity of operation within the wide input voltage and power range without losing stability.

Table III: Experimental measurement of the PV energy conversion efficiency

Profile	Microinverter type											
	LoMI				HiMI				STMI			
	MPP	η_{MPPT} [%]	η_{MI} [%]	η_{PV} [%]	MPP	η_{MPPT} [%]	η_{MI} [%]	η_{PV} [%]	MPP	η_{MPPT} [%]	η_{MI} [%]	η_{PV} [%]
ST-1	MPP1	77	92.3	71.1	MPP1	77	94.9	73.1	MPP2	97	90.5	**87.8**
ST-2	MPP1	79	92.9	73.4	MPP1	79	95.3	75.3	MPP2	99	91.6	**90.7**
G-1	MPP1	68	93.2	63.4	MPP2	99	95.7	**94.7**	MPP2	99	94	93.1
G-2	MPP1	44	93.0	40.9	MPP2	55	95.6	52.6	MPP4	99	91.5	**90.6**
GBS-1	MPP1	62	91.9	57	MPP2	75.5	95.3	72	MPP4	99	85.5	**84.6**
GBS-2	MPP1	91	94.1	85.6	MPP2	99	95.5	**94.5**	MPP2	99	91.5	90.6

Table IV: Experimental efficiency of STMI operating with different BIPV microstrings

Type of BIPV roof module	Number of elements within a BIPV microstring								
	1	2	3	4	5	6	7	8	9
Gaia GS Integra Line SP 595	-	82.9% 80 W*	87.5% 120 W	91% 160 W	92.5% 200 W	93.8% 240 W	95.1% 280 W	93% 320 W	92% 360 W
SunTegra® Shingle	86% 105 W	92.7% 210 W	92.9% 315 W	-					
GB-Sol PV Slate	-	85% 70 W	89.9% 105 W	92% 140 W	94.6% 175 W	94.2% 210 W	94% 245 W	-	

* The lowest voltage of the BIPV microstring used in these tests equals 9.6 V

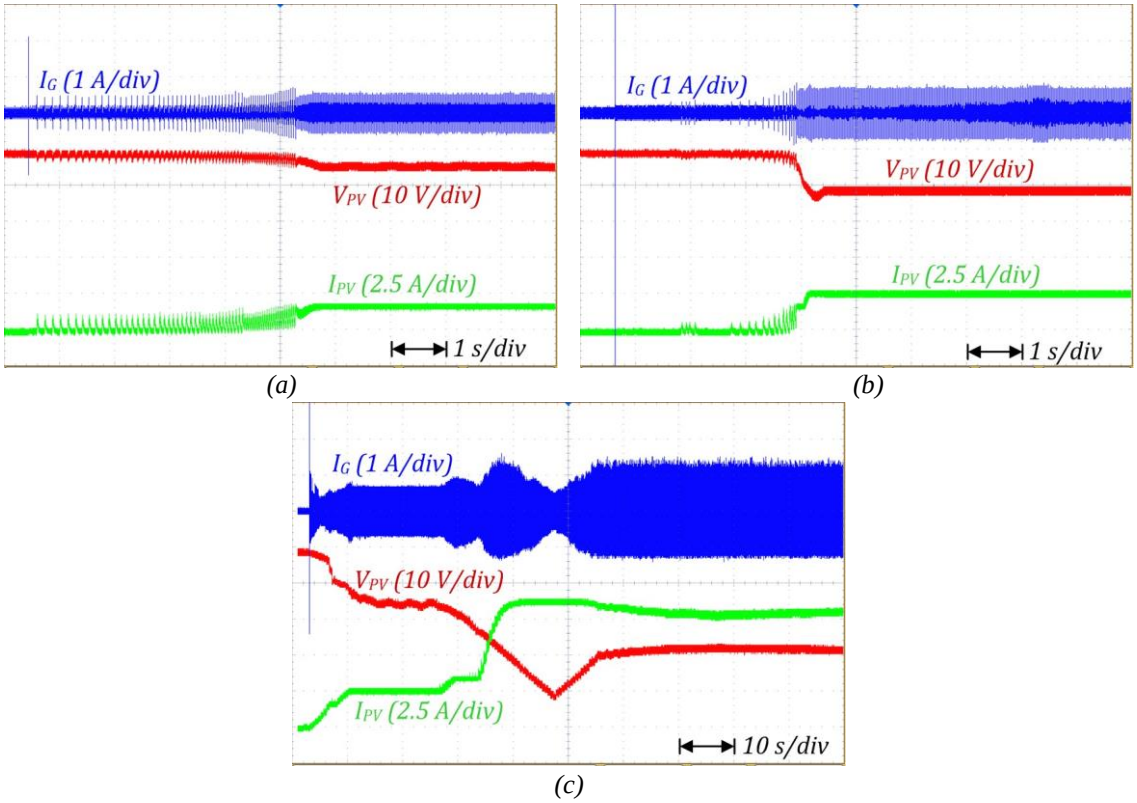

Fig. 9: Strat-up and MPPT of the LoMI (a), HiMI (b) and STMI (c) with PV profile G-2 (I_G – grid current, V_{PV} – input voltage, I_{PV} – input current).

Conclusions

This paper introduces the concept of application of PV microinverters to BIPV solar roofs. However, the available commercial microinverters based on single-stage interleaved flyback converter topology feature narrow maximum power point tracking range that limits their application flexibility in BIPV solar roofs. To resolve this limitation, the shade-tolerant microinverter (STMI) concept named Optiverter was justified as a solution for the building integrated PV solar roofs where roofing elements are connected in microstrings for their further parallel grid integration. The Optiverter enables shade tolerant (global) maximum point tracking and by this means, provides superior performance under partial shading conditions that are often present in the residential buildings, especially in the urban areas. The STMI performs P-V curve scanning and thus can define the global maximum power point.

Moreover, it post-processes found local and global maximum power points by applying look-up table of the STMI efficiency. As a result, the control system defines the maximum power point with the maximum output power that could be different from the global maximum power point of a microstring. The experimental results prove that the Optiverter is superior to the existing commercial microinverters: it is compatible with much wider variety of BIPV microstring configurations; it is rated for higher power to adopt rising efficiency of modern Si-based PV cells; it can provide MPPT efficiency approaching 100% under shading conditions; intelligent control system maximizes the PV power production. The future research on Optiverter will address several challenges identified: relatively low efficiency at low input voltage will be improved by application of the novel multi-mode control method with variable DC-link voltage, frequency and duration of P-V curve rescanning will be optimized to achieve the trade-off between energy yield and stability of the control system.

References

[1] Gillingham K., Rapsony D., Wagner G.: The rebound effect and energy efficiency policy, Review of Environmental Economics and Policy, vol. 10, no. 1, pp. 68–88, 2016.

[2] Ellabban O., Abu-Rub H., Blaabjerg F.: Renewable energy resources: Current status, future prospects and their enabling technology, Renewable and Sustainable Energy Reviews, vol. 39, pp. 748 764, 2014.

[3] Bose K. B.: Global Energy Scenario and Impact of Power Electronics in 21st Century, IEEE Transactions on Industrial Electronics, vol. 60, no. 7, July 2013.

[4] Nejat P., et al, A global review of energy consumption, CO2 emissions and policy in the residential sector, Renewable and Sust. Energy Reviews, vol. 43, pp. 843-862, 2015.

[5] Soares N., Bastos J., Dias Pereira L., Soares A. et al: A review on current advances in the energy and environmental performance of buildings towards a more sustainable built environment, Renewable and Sustainable Energy Reviews, vol. 77, pp. 845-860, 2017.

[6] Kyle P., Clarke L., Rong F. et al: Climate policy and the long-term evolution of the U.S. buildings sector, Energy Journal, vol. 31, no. 3, pp. 131 158, 2010.

[7] European Parliament and Council: Directive 2010/31/EU of the European Parliament and of the Council of 19 May 2010 on the energy performance of buildings, Official J. of the European Union, L153, pp. 13-35, 2010.

[8] Kurnitski J., Saari A., Kalamees T., Vuolle M. et al: Cost optimal and nearly zero (nZEB) energy performance calculations for residential buildings with REHVA definition for nZEB national implementation, Energy and Buildings, vol. 43, no. 11, pp. 3279-3288, 2011.

[9] Marszal A. J., Heiselberg P., Jensen R. L., Norgaard J.: On-site or off-site renewable energy supply options? Life cycle cost analysis of a Net Zero Energy Building in Denmark, Renewable Energy, vol. 44, pp. 154-165, 2012.

[10] Bruni G., et al.: Domestic distributed power generation: Effect of sizing and energy management strategy on the environmental efficiency of a photovoltaic-battery-fuel cell system, Energy, vol. 77, pp. 133-143, 2014.

[11] Tripathy M., Sadhu P. K., Pandab S. K.: A critical review on building integrated photovoltaic products and their applications, Renewable and Sustainable Energy Reviews, vol. 61, pp. 451 465, Aug. 2016.

[12] D. Iannuzzi, L. Piegari and P. Tricoli, "A novel PV-modular multilevel converter for building integrated photovoltaics," In Proc. EVER'2013, Monte Carlo, 2013, pp. 1-7.

[13] B. Liu, S. Duan and T. Cai: Photovoltaic DC-Building-Module-Based BIPV System—Concept and Design Considerations, IEEE Transactions on Power Electronics, vol. 26, no. 5, pp. 1418-1429, May 2011.

[14] S.W.H. de Haan, H. Oldenkamp, C.F.A. Frumau and W. Bonin: Development of a 100Wresonant inverter for AC modules, Proceedings of 12th EPSEC, Amsterdam, The Netherlands, 1994.

[15] A. Lohner, T. Meyer and A. Nagel: A new panel-integratable inverter concept for grid-connected photovoltaic systems, Proc. of IEEE Int. Symposium on Ind. Electronics, Warsaw, 1996, vol.2, pp. 827-831.

[16] U. Herrmann, H. G. Langer and H. van der Broeck: Low cost DC to AC converter for photovoltaic power conversion in residential applications, Proceedings PESC'93, Seattle, WA, 1993, pp. 588-594.

[17] D. Vinnikov, R. Kosenko, A. Chub and E. Liivik: Shade-tolerant photovoltaic microinverter with time adaptive seamless P-V curve sweep MPPT, in Proc. EPE'17 ECCE Europe, Warsaw, 2017, pp. 1-8.